An Improved Adaptive Sidelobe Blanker

Francesco Bandiera, *Member, IEEE*, Olivier Besson, *Senior Member, IEEE*, Danilo Orlando, and Giuseppe Ricci, *Member, IEEE*

***Abstract*—We propose a two-stage detector consisting of a subspace detector followed by the whitened adaptive beamformer orthogonal rejection test. The performance analysis shows that it possesses the constant false alarm rate property with respect to the unknown covariance matrix of the noise and that it can guarantee a wider range of directivity values with respect to previously proposed two-stage detectors. The probability of false alarm and the probability of detection (for both matched and mismatched signals) have been evaluated by means of numerical integration techniques.**

***Index Terms*—Adaptive radar detection, adaptive sidelobe blanker, constant false alarm rate (CFAR), mismatched signals.**

I. Introduction

In the last decades several papers have addressed adaptive radar detection of targets embedded in Gaussian or non-Gaussian disturbance. Most of these papers follow the lead of the seminal paper by Kelly [1], where the generalized likelihood ratio test (GLRT) is used to conceive an adaptive decision scheme capable of detecting coherent pulse trains in presence of Gaussian disturbance with unknown spectral properties. In [2], it is shown that an ad hoc detector, based on the two-step GLRT-based design procedure and referred to in the following as adaptive matched filter (AMF), can also achieve better probability of detection than Kelly's detector for high signal-to-noise ratios (SNRs). The tools of invariance have been used in [3] to address adaptive detection in presence of structured and unstructured disturbance. Detection of point-like targets in non-Gaussian noise has been dealt with in ([4] and references therein). The case of point-like targets assumed to belong to a known subspace of the observables has been addressed in [5] and [6]. The case of rank-one waveforms that are only partially known has been dealt with in [7]; therein, the invariance properties of the decision problem are studied and the corresponding maximal invariant is derived. Finally, the authors design the GLRT-based detector for the problem at hand. In addition, several detection algorithms for point-like or extended targets embedded in Gaussian disturbance are encompassed as special cases of the amazingly general framework and derivation described in [8].

All of the above papers assume that returns from the target can be modeled in terms of (a linear combination of) deterministic signals known up to multiplicative, possibly complex, constants, taking into account both target and channel effects. Moreover, those detectors rely on the assumption that a set of secondary data, namely returns free of signals components, but sharing the spectral properties of the noise in the data under test, is available. Such secondary data are used to come up with fully adaptive detection schemes.

It is also important to stress that most detectors have not been designed to distinguish between mainlobe and sidelobe mismatched signals. As a matter of fact, the actual signal backscattered from a target (or target's scattering centers) can be different from the nominal one and the mismatch can have different reasons as, for example [9], [10], the following:

- coherent scattering from a direction different to that in which the radar system is steered (sidelobe target);
- imperfect modeling of the mainlobe target by the nominal steering vector, where the mismatch may be due to multipath propagation, array calibration uncertainties, beampointing errors, etc.

Thus, it might be important to trade detection performance of mainlobe targets for rejection capabilities of sidelobe ones. In order to face with this dilemma, the adaptive beamformer orthogonal rejection test (ABORT) detector was introduced in [9]. The idea of ABORT is to modify the null hypothesis, which usually states that the vector under test contains noise only, so that it possibly contains a vector which, in some way, is orthogonal to the assumed target's signature. Doing so, if a signal with actual steering vector different from the nominal one is present, the detector will be less inclined to declare a detection, as the null hypothesis will be more plausible. For instance, if a sidelobe target is present, the ABORT detector will exhibit less false alarms than detectors, which are rather sensitive to mismatched signals, as the AMF. As customary, it is assumed that a set of secondary data is available at the receiver. The directivity of such detector is in between that of Kelly's detector (which, in turn, is more directive than the AMF) and the one of the adaptive coherence estimator (ACE) [4], [5].

However, in the original ABORT formulation, the fictitious signal under the null hypothesis was assumed to be orthogonal to the nominal one, in the *quasi-whitened* space, i.e., after whitening by the sample covariance matrix of the training samples. In [11], such an assumption was modified to address adaptive detection of distributed targets embedded in homogeneous disturbance, by resorting to the GLRT with the useful and the

Manuscript received August 9, 2007; revised April 19, 2008. First published May 28, 2008; last published August 13, 2008 (projected). The associate editor coordinating the review of this manuscript and approving it for publication was Dr. Erchin Serpedin. The work of O. Besson was supported by the Mission pour la Recherche et l'Innovation Scientifique (MRIS) of the Délégation Générale pour l'Armement (DGA) by Grant 06-60-034.

F. Bandiera, D. Orlando, and G. Ricci are with the Dipartimento di Ingegneria dell'Innovazione, Università del Salento, 73100 Lecce, Italy (e-mail: francesco.bandiera@unile.it; danilo.orlando@unile.it; giuseppe.ricci@unile.it).

O. Besson is with the Department of Electronics, Optronics and Signal, University of Toulouse, ISAE, BP 54032–31055 Toulouse, Cedex 4, France (e-mail: besson@isae.fr).

Digital Object Identifier 10.1109/TSP.2008.926191

fictitious signals orthogonal in the *whitened* space, i.e., after whitening with the true covariance matrix. This seemingly minor modification led to significant differences compared to ABORT and, more particularly, to an enhanced rejection of sidelobe signals. Furthermore, in [11], it is shown that such detector, referred to in the following as whitened ABORT (W-ABORT), may become even more selective than the ACE.

On the other hand, increased robustness can be achieved by resorting to the tools of subspace detection, namely assuming that the target belongs to a known subspace of the observables, or also constraining the possible useful signals to belong to a proper cone with axis the whitened nominal steering vector [12], [13]. Moreover, extending such a cone idea by modeling the null hypothesis as the complement of a cone to the entire space of the observables leads to a family of detectors capable of trading detection performance of mainlobe targets for rejection capabilities of sidelobe ones. A way to combine the ABORT rationale with the subspace idea has been dealt with in [10] as a possible means to retain an acceptable detection loss for slightly mismatched mainlobe targets.

Another class of detectors that combines the statistics of Kelly's detector and of the AMF has been proposed by Kalson [14]: the detector statistic depends on a design parameter $\alpha \in [0,1]$ that allows to obtain receiver operating characteristics, actually the probability of detection (P_d) versus the SNR, in between that of Kelly's detector and the one of the AMF.

Unfortunately, though, it seems difficult to find a decision scheme capable of providing at the same time good capabilities to reject sidelobe targets and high power in case of slightly mismatched mainlobe targets. In order to face with this problem, the so-called *two-stage detectors* have been proposed; such schemes are formed by cascading two detectors (usually with opposite behaviors): the overall one declares the presence of a target in the data under test only when data under test survive both detection thresholdings. A rather famous two-stage detector is the adaptive sidelobe blanker (ASB). The ASB has been proposed as a means for mitigating the high number of false alarms of the AMF in the presence of undernulled interference [15]–[17]. It can be seen as the cascade of the AMF and the ACE. Remarkably, it can adjust directivity by proper selection of the two thresholds in order to trade good rejection capabilities of sidelobe targets for an acceptable detection loss of matched signals [18], [19]. Richmond has also provided analytical expressions for the P_d and the probability of false alarm $(P_{\rm fa})$ of the ASB and demonstrated that, in homogeneous environment and with matched signals, it has higher or commensurate P_d, for a given $P_{\rm fa}$, than both the AMF and the ACE and an overall performance that is commensurate with Kelly's detector [20]. A further two-stage detector, consisting of the cascade of the AMF and Kelly's detector, has been proposed as a computationally efficient implementation of the latter [19]. Moreover, in [21], a two-stage detector obtained cascading a RAO test to the AMF has been proposed and assessed. Note that the above two-stage detectors are invariant to the group of transformations given in [3].

More recently, another two-stage detector, the so-called *subspace-based ASB* (S-ASB), has been proposed [22]. Specifically, the S-ASB is obtained cascading a subspace GLRT-based detector [referred to in the following as subspace detector (SD)] and the ACE; the performance assessment has shown that such solution can increase the robustness of the composite detector while retaining the same selectivity of the ASB. However, it is not invariant to the group of transformations given in [3]. Based upon the experience of [22], herein we propose a two-stage detector aimed at increasing also the selectivity of the S-ASB, i.e., the capability to reject mismatched signals. This is accomplished by cascading the SD and the W-ABORT. The performance assessment confirms that its directivity varies in a wider range than its competitors, at least for the considered class of mismatched signals, when we constrain the maximum loss with respect to Kelly's detector for matched signals, given $P_{\rm fa}$ and P_d.

The remainder of the paper is organized as follows. The next section is devoted to the problem formulation and to the description of the proposed detector while Section III contains its performance assessment; to this end, we derive analytical expressions for $P_{\rm fa}$ and P_d (for matched and mismatched signals). In Section IV, we report some illustrative examples in which we compare the performance of the proposed detector with those of the S-ASB, ASB, and of the two-stage detector proposed in [21]. Concluding remarks are given in Section V. Finally, Appendixes A and B contain some analytical derivations.

II. Problem Formulation

Assume that a linear array formed by N_a antennas senses the cell under test and that each antenna collects N_t samples. Denote by $\boldsymbol{z} \in \mathbb{C}^{N\times 1}$ the N-dimensional column vector, with $N = N_a N_t$, containing returns from the cell under test. We want to test whether or not $\boldsymbol{z}$ contains useful target echoes. As customary, we assume that a set of K secondary data, $\boldsymbol{z}_k \in \mathbb{C}^{N\times 1}$, $k = 1,\ldots,K$, $K \geq N$, namely data free of signal components but sharing the same statistical properties of the noise in the cell under test, is available.

The detection problem can be recast as

$$\begin{cases} H_0 : \begin{cases} \boldsymbol{z} = \boldsymbol{n}, \\ \boldsymbol{z}_k = \boldsymbol{n}_k, \end{cases} & k = 1,\ldots,K \\ H_1 : \begin{cases} \boldsymbol{z} = \alpha \boldsymbol{p} + \boldsymbol{n}, \\ \boldsymbol{z}_k = \boldsymbol{n}_k, \end{cases} & k = 1,\ldots,K \end{cases}$$

where the following holds:

- $\boldsymbol{n}$ and the $\boldsymbol{n}_k \in \mathbb{C}^{N\times 1}$, $k = 1,\ldots,K$, are independent and identically distributed complex normal random vectors with zero-mean and unknown, positive-definite covariance matrix $\boldsymbol{R} \in \mathbb{C}^{N\times N}$, i.e., $\boldsymbol{n}, \boldsymbol{n}_k \sim \mathcal{CN}_N(\boldsymbol{0}, \boldsymbol{R})$, $k = 1,\ldots,K$;
- $\boldsymbol{p} \in \mathbb{C}^{N\times 1}$ is the direction of the (possible) mainlobe target echo, possibly different from that of the nominal steering vector $\boldsymbol{v}_0 \in \mathbb{C}^{N\times 1}$;
- $\alpha \in \mathbb{C}$ is an unknown (deterministic) factor which accounts for both target and channel effects.

In the following we propose and assess a two-stage detector obtained by cascading the SD [8], whose statistic is given by

$$t_{\mathrm{SD}} = \frac{\boldsymbol{z}^{\dagger}\boldsymbol{S}^{-1}\boldsymbol{H}(\boldsymbol{H}^{\dagger}\boldsymbol{S}^{-1}\boldsymbol{H})^{-1}\boldsymbol{H}^{\dagger}\boldsymbol{S}^{-1}\boldsymbol{z}}{1+\boldsymbol{z}^{\dagger}\boldsymbol{S}^{-1}\boldsymbol{z}} \tag{1}$$

and the W-ABORT, whose statistic is given by [11]

$$t_{\mathrm{WA}} = \frac{1}{\left[\dfrac{|\boldsymbol{z}^{\dagger}\boldsymbol{S}^{-1}\boldsymbol{v}_0|^2}{(1+\boldsymbol{z}^{\dagger}\boldsymbol{S}^{-1}\boldsymbol{z})(\boldsymbol{v}_0^{\dagger}\boldsymbol{S}^{-1}\boldsymbol{v}_0)}-1\right]^2(1+\boldsymbol{z}^{\dagger}\boldsymbol{S}^{-1}\boldsymbol{z})} \tag{2}$$

where the following holds:

- † denotes conjugate transpose;
- $\boldsymbol{S} \in \mathbb{C}^{N\times N}$ is K times the sample covariance matrix of the secondary data, i.e., $\boldsymbol{S} = \boldsymbol{Z}\boldsymbol{Z}^{\dagger}$ with $\boldsymbol{Z} = [\boldsymbol{z}_1 \cdots \boldsymbol{z}_K] \in \mathbb{C}^{N\times K}$;
- $\boldsymbol{H} \in \mathbb{C}^{N\times r}$ is a full-column-rank matrix (and, hence, $r \geq 1$ is the rank of $\boldsymbol{H}$). Hereafter, we assume that the first column of $\boldsymbol{H}$ is $\boldsymbol{v}_0$, i.e., $\boldsymbol{H} = [\boldsymbol{v}_0\, \boldsymbol{v}_1 \cdots \boldsymbol{v}_{r-1}]$, and defer to Section IV the choice of the remaining columns of $\boldsymbol{H}$.

Notice that

$$t_{\mathrm{K}} = \frac{|\boldsymbol{z}^{\dagger}\boldsymbol{S}^{-1}\boldsymbol{v}_0|^2}{(1+\boldsymbol{z}^{\dagger}\boldsymbol{S}^{-1}\boldsymbol{z})(\boldsymbol{v}_0^{\dagger}\boldsymbol{S}^{-1}\boldsymbol{v}_0)}$$

is the well-known decision statistic of Kelly's detector [1].

Summarizing, the operation of the newly-proposed detector, referred to in the following as WAS-ASB, can be pictorially described as follows:

$$t_{\mathrm{SD}} \underset{H_0}{\overset{H_1}{\gtrless}} \eta \quad \rightarrow \quad t_{\mathrm{WA}} \underset{H_0}{\overset{H_1}{\gtrless}} \xi \quad \rightarrow H_1$$

where η and ξ form the threshold pair to be set in order to guarantee the overall desired P_{fa}.

III. Performance Assessment

In this section, we derive analytical expressions for P_d and P_{fa} of the WAS-ASB; to this end, we replace t_{SD} with the equivalent decision statistic $\tilde{t}_{\mathrm{SD}} = 1/(1-t_{\mathrm{SD}})$. Based upon results contained in [22], it is possible to show that $\tilde{t}_{\mathrm{SD}}$ and t_{WA} admit the following stochastic representations:

$$\tilde{t}_{\mathrm{SD}} = (\tilde{t}_{\mathrm{K}}+1)(1+c)$$
$$t_{\mathrm{WA}} = \frac{(\tilde{t}_{\mathrm{K}}+1)}{(1+b)(1+c)}$$

where $\tilde{t}_{\mathrm{K}} = t_{\mathrm{K}}/(1-t_{\mathrm{K}})$ (see Appendix A).

Moreover, under the H_0 hypothesis:

- $\tilde{t}_{\mathrm{K}}$, given b and c, is ruled by the complex central F-distribution with 1, $K-N+1$ degrees of freedom [8] (for a definition of complex normal related statistics, see also [20, App. A]);
- b is a complex central F-distributed random variable (rv) with $N-r$, $K-N+r+1$ degrees of freedom, i.e., $b \sim \mathcal{CF}_{N-r,K-N+r+1}$ (see [22, App. B]);
- $c \sim \mathcal{CF}_{r-1,K-N+2}$ (see [22, App. B]);
- b and c are statistically independent rv's (see [22, App. B]).

Now, the P_{fa} of the two-stage detector can be expressed as

$$\begin{aligned}
P_{\mathrm{fa}}(\eta,\xi) &= \mathrm{P}[t_{\mathrm{SD}} > \eta, t_{\mathrm{WA}} > \xi; H_0] \\
&= \mathrm{P}[\tilde{t}_{\mathrm{SD}} > \tilde{\eta}, t_{\mathrm{WA}} > \xi; H_0] \\
&= \mathrm{P}\left[(\tilde{t}_{\mathrm{K}}+1)(1+c) > \tilde{\eta}, \frac{\tilde{t}_{\mathrm{K}}+1}{(1+c)(1+b)} > \xi; H_0\right] \\
&= 1 - \mathrm{P}\left[\tilde{t}_{\mathrm{K}} \leq \max\left(\frac{\tilde{\eta}}{1+c}-1,\right.\right. \\
&\qquad \left.\left.\xi(1+b)(1+c)-1\right); H_0\right] \\
&= 1 - \int_0^{+\infty}\int_0^{+\infty} \mathrm{P}\left[\tilde{t}_{\mathrm{K}} \leq \max\left(\frac{\tilde{\eta}}{1+\gamma}\right.\right. \\
&\qquad \left.\left. -1, \xi(1+\beta)(1+\gamma)-1\right) | b=\beta, c=\gamma; H_0\right] \\
&\qquad \times p_b(\beta)p_c(\gamma)d\beta d\gamma \\
&= 1 - \int_0^{+\infty}\int_0^{+\infty} \mathcal{P}_0\left(\max\left(\frac{\tilde{\eta}}{1+\gamma}-1,\right.\right. \\
&\qquad \left.\left.\xi(1+\beta)(1+\gamma)-1\right)\right) p_b(\beta)p_c(\gamma)d\beta d\gamma
\end{aligned}$$

where $\tilde{\eta} = 1/(1-\eta)$, $p_b(\cdot)$ is the probability density function (pdf) of the rv $b \sim \mathcal{CF}_{N-r,K-N+r+1}$, $p_c(\cdot)$ is the pdf of the rv $c \sim \mathcal{CF}_{r-1,K-N+2}$, and $\mathcal{P}_0(\cdot)$ is the cumulative distribution function (CDF) of the rv $\tilde{t}_{\mathrm{K}}$, given b and c (and under H_0), i.e., the CDF of a rv ruled by the $\mathcal{CF}_{1,K-N+1}$ distribution.

The following remarks are now in order. First, it is apparent that the WAS-ASB possesses the constant false alarm rate (CFAR) property with respect to $\boldsymbol{R}$. Second, note that the P_{fa} of the two-stage detector depends on two thresholds; as a consequence, there exist infinite threshold pairs that guarantee the same value of P_{fa}. Third, observe that the P_{fa} is independent of $\boldsymbol{H}$ but for the value of r (and provided that the first column of $\boldsymbol{H}$ is $\boldsymbol{v}_0$). For the reader's ease, Fig. 1 shows the contour plots for the WAS-ASB corresponding to different values of P_{fa}, as functions of the threshold pairs $(\xi,\tilde{\eta})$, $N=16$, $K=32$, and $r=2$. All curves have been obtained by means of numerical integration techniques. Note that, for a preassigned P_{fa}, the threshold of the SD does not approximately change for values of the threshold of the W-ABORT ranging from 0 to 0.2.

Under the H_1 hypothesis, we assume a misalignment between the actual steering vector $\boldsymbol{p}$ and the nominal one $\boldsymbol{v}_0$, i.e., $\boldsymbol{p} \neq \boldsymbol{v}_0$. In this case, the rv's b and c depend on $\cos^2\theta$ defined through (5) of Appendix B; for this reason, in the following, we will denote these rv's by b_θ and c_θ. Due to the useful signal components, the distributions of $\tilde{t}_{\mathrm{K}}$, b_θ, and c_θ change, more precisely (see Appendix B):

- $\tilde{t}_K$, given b_θ and c_θ, is ruled by the complex noncentral F-distribution with $1, K-N+1$ degrees of freedom and noncentrality parameter

$$\delta_\theta^2 = \frac{\mathrm{SNR}\cos^2\theta}{(1+b_\theta)(1+c_\theta)}$$

where

$$\mathrm{SNR} = |\alpha|^2\boldsymbol{p}^{\dagger}\boldsymbol{M}^{-1}\boldsymbol{p}$$

is the total available signal-to-noise ratio;

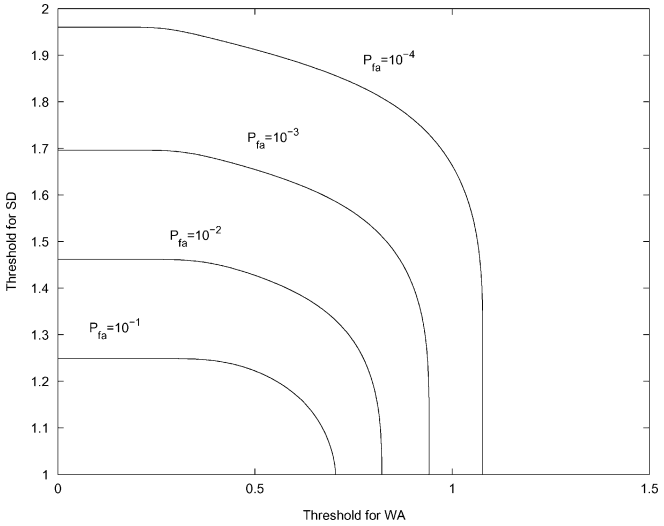

Fig. 1. Contours of constant $P_{\rm fa}$ for the WAS-ASB with $N = 16$, $K = 32$, and $r = 2$.

- b_θ is ruled by the complex noncentral F-distribution with $N-r, K-N+r+1$ degrees of freedom and noncentrality parameter

$$\delta_{b_\theta}^2 = \mathrm{SNR}\ \sin^2\theta\ \|\boldsymbol{h}_{B_1}\|^2$$

  i.e., $b_\theta \sim \mathcal{CF}_{N-r,K-N+r+1}(\delta_{b_\theta})$, where $\boldsymbol{h}_{B_1}$ is defined in Appendix B;
- given b_θ, $c_\theta \sim \mathcal{CF}_{r-1,K-N+2}(\delta_{c_\theta})$, with

$$\delta_{c_\theta}^2 = \frac{\mathrm{SNR}\ \sin^2\theta\ \|\boldsymbol{h}_{B_0}\|^2}{1+b_\theta}$$

  where $\boldsymbol{h}_{B_0}$ is defined in Appendix B.

Thus, proceeding along the same line as for the derivation of the $P_{\rm fa}$, it is easy to see that the P_d is given by

$$\begin{aligned}
&P_d(\mathrm{SNR},\eta,\xi,\cos^2\theta,\|\boldsymbol{h}_{B_0}\|,\|\boldsymbol{h}_{B_1}\|)\\
&= \mathrm{P}[t_{\rm SD} > \eta, t_{\rm WA} > \xi; H_1]\\
&= \mathrm{P}[\tilde{t}_{\rm SD} > \tilde{\eta}, t_{\rm WA} > \xi;\ H_1]\\
&= \mathrm{P}\left[(1+c_\theta)(\tilde{t}_{\rm K}+1) > \tilde{\eta}, \frac{\tilde{t}_{\rm K}+1}{(1+b_\theta)(1+c_\theta)} > \xi; H_1\right]\\
&= 1 - \int_0^{+\infty}\int_0^{+\infty} \mathcal{P}_1\left(\max\left(\frac{\tilde{\eta}}{1+\gamma}-1, \xi(1+\beta)(1+\gamma)-1\right)\right)\\
&\quad \times p_{b_\theta c_\theta}(\beta,\gamma)\, d\beta\, d\gamma\\
&= 1 - \int_0^{+\infty}\int_0^{+\infty} \mathcal{P}_1\left(\max\left(\frac{\tilde{\eta}}{1+\gamma}-1, \xi(1+\beta)(1+\gamma)-1\right)\right)\\
&\quad \times p_{c_\theta|b_\theta}(\gamma|b_\theta=\beta)\, p_{b_\theta}(\beta)\, d\beta\, d\gamma, \qquad (3)
\end{aligned}$$

where $\mathcal{P}_1(\cdot)$ is the CDF of the rv $\tilde{t}_{\rm K}$, given b_θ and c_θ (and under H_1), i.e., the CDF of a rv ruled by the $\mathcal{CF}_{1,K-N+1}(\delta_\theta)$ distribution, $p_{b_\theta}(\cdot)$ is the pdf of a rv ruled by the $\mathcal{CF}_{N-r,K-N+r+1}(\delta_{b_\theta})$, and $p_{c_\theta|b_\theta}(\cdot|\cdot)$ is the pdf of a rv ruled by the $\mathcal{CF}_{r-1,K-N+2}(\delta_{c_\theta})$.

In the case of perfect match between $\boldsymbol{v}_0$ and $\boldsymbol{p}$, i.e., $\theta = 0$, δ_{b_θ} and δ_{c_θ} are equal to zero, thus rv's c_θ and b_θ obey to the complex central F-distributions with $N-r, K-N+r+1$ and $r-1, K-N+2$ degrees of freedom, respectively. On the other hand, $\tilde{t}_{\rm K}$ is still subject to the complex noncentral F-distribution with $1, K-N+1$ degrees of freedom and noncentrality parameter given by

$$\delta_0^2 = \frac{\mathrm{SNR}}{(1+b_0)(1+c_0)}$$

and (in this case) the P_d does not depend on the choice of $\boldsymbol{H}$ but for the value of r (and provided that the first column of $\boldsymbol{H}$ is $\boldsymbol{v}_0$).

IV. Illustrative Examples and Discussion

In this section, we present some numerical examples to show the effectiveness of the WAS-ASB, also in comparison to the ASB, the S-ASB, and the two-stage detector proposed in [21] and referred to in the following as AMF-RAO. All curves have been obtained by means of numerical integration techniques[1]. In all examples, the noise is modeled as an exponentially-correlated complex normal vector with one-lag correlation coefficient ρ, namely the (i,j)th element of the covariance matrix $\boldsymbol{R}$ is given by $\rho^{|i-j|}$, $i,j = 1,\ldots,N$, with $\rho = 0.95$. The probability of false alarm is set to 10^{-4}. Moreover, we set $N_t = 1$, $N_a = N$, and choose $\boldsymbol{v}_0 = \boldsymbol{s}(0)$ with

$$\boldsymbol{s}(\phi) = \frac{1}{\sqrt{N}}\left[1\ e^{j\frac{2\pi d}{\lambda}\sin\phi}\ \cdots\ e^{j(N-1)\frac{2\pi d}{\lambda}\sin\phi}\right]^T$$

where d is the interelement spacing, λ is the radar operating wavelength, and ^{T} denotes transpose. Moreover, we will denote by ϕ_T the azimuthal angle of the impinging useful target echo, i.e., $\boldsymbol{p} = \boldsymbol{s}(\phi_T)$.

Until now, we have left aside the problem of how to choose r and the remaining columns of $\boldsymbol{H}$. First, remember that, under matching conditions, P_d does not depend on the choice of $\boldsymbol{H}$ but for the value of r. However, the design of $\boldsymbol{H}$ will impact on the performance of the detector in presence of mismatched signals. In fact, values of r greater than one are necessary to increase its robustness. The design of $\boldsymbol{H}$ is a challenging problem: simulation results not reported herein indicate that values of $r > 2$ or $r = 2$ and a vector $\boldsymbol{v}_1$ significantly mismatched with respect to $\boldsymbol{v}_0$ may produce curves of P_d versus ϕ_T whose transition from the "bandpass" to the "stopband" is not sharp; see [22] for a more detailed discussion about this issue. For this reason, in the following we set $r = 2$ and $\boldsymbol{v}_1 = \boldsymbol{s}(\phi_1)$, with $\phi_1 = \pi/360$, and discuss the behavior of the corresponding detector in order to prove its effectiveness.

In Figs. 2–4, we plot P_d versus SNR for the S-ASB, the WAS-ASB, and the AMF-RAO, respectively, as they compare to Kelly's detector [1], for the case of a matched target, $N = 16$, $K = 32$; in these figures, we show two curves (in addition to the curve of Kelly's detector) for each of them: such curves correspond to the limiting behaviors of the two-stage detectors for

[1]For the WAS-ASB, we also show results obtained through Monte Carlo simulation. To this end, we resorted to $100/P_{\rm fa}$ and 10^4 independent trials in order to evaluate the thresholds necessary to ensure a preassigned value of $P_{\rm fa}$ and the P_d's, respectively. Simulated results are presented in Figs. 3 and 7 and are shown as cross markers.

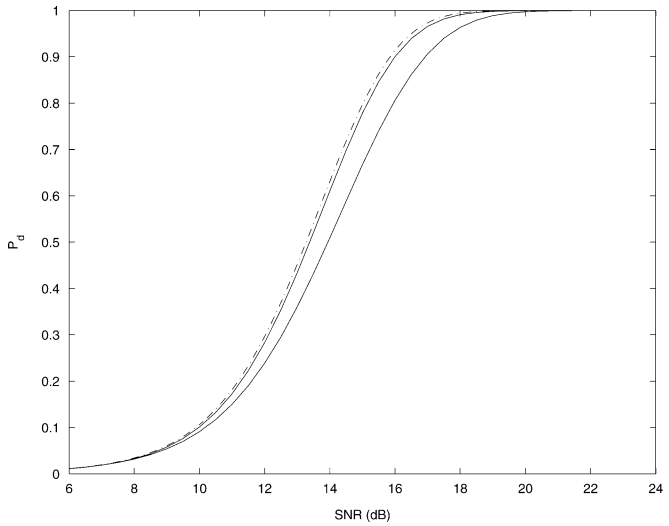

Fig. 2. P_d versus SNR for the S-ASB (solid lines) and Kelly's detector (dashed–dotted line) with $N = 16$, $K = 32$, and $r = 2$.

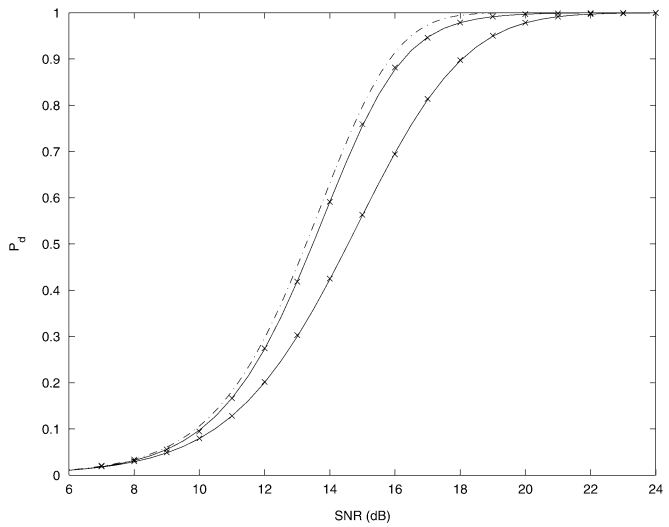

Fig. 3. P_d versus SNR for the WAS-ASB (solid lines) and Kelly's detector (dashed–dotted line) with $N = 16$, $K = 32$, and $r = 2$. Cross markers denote results obtained by Monte Carlo simulation.

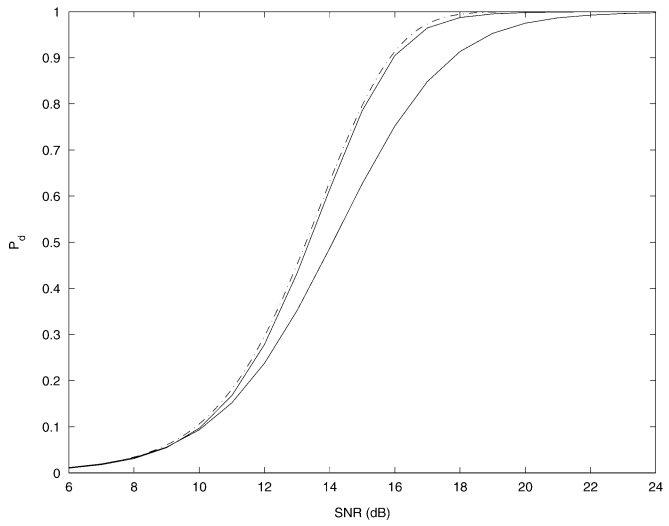

Fig. 4. P_d versus SNR for the AMF-RAO (solid lines) and Kelly's detector (dashed–dotted line) with $N = 16$ and $K = 32$.

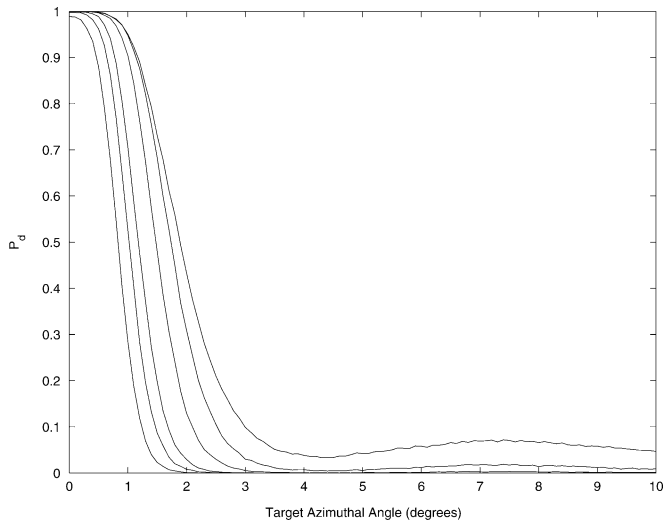

Fig. 5. P_d versus target azimuthal angle for the ASB with $N = 16$, $K = 32$, and $\mathrm{SNR} = 19$ dB.

threshold settings which guarantee $P_{\mathrm{fa}} = 10^{-4}$. Fig. 2 shows that the maximum loss of the S-ASB with respect to Kelly's detector is less than (about) 1.2 dB (at $P_d = 0.9$); such a maximum loss increases to (about) 2 dB in Figs. 3 and 4 for the WAS-ASB and the AMF-RAO.

In Figs. 5–8, we plot P_d versus ϕ_T (measured in degrees) for the ASB, the S-ASB, the WAS-ASB, and the AMF-RAO, respectively, $N = 16$, $K = 32$; all plotted curves refer to those threshold pairs which ensure the best rejection capabilities of sidelobe targets under the constraint that the loss with respect to Kelly's detector and for matched signals is less than (about) 1 dB at $P_d = 0.9$ and $P_{\mathrm{fa}} = 10^{-4}$. Observe from Figs. 5 and 6 that the S-ASB can ensure better robustness with respect to the ASB, due to the first stage (the SD), which is less sensitive than the AMF to mismatched signals. However, S-ASB and ASB exhibit the same capability to reject sidelobe targets, according to the fact that the second stage (the ACE) is the same. As it can be seen from Figs. 6 and 7, instead, the WAS-ASB guarantees the same robustness of the S-ASB, but better rejection capabilities than the latter (and, consequently, better rejection capabilities than the ASB), due to the fact that the ACE has been replaced by the W-ABORT. Other simulation results not reported here, in order not to burden too much the analysis, have shown that the WAS-ASB is generally more selective than the ASB and the S-ASB and more robust than the ASB. Finally, from Figs. 7 and 8, we see that the AMF-RAO is slightly more selective than the WAS-ASB for the considered parameter values.

In Figs. 9 and 10, we plot contours of constant P_d, as functions of SNR and $\cos^2\theta$; as for the curves of Figs. 5–8, thresholds are such that the loss with respect to Kelly's detector is less than (about) 1 dB for the perfectly matched case. More precisely, in Fig. 9, we analyze the robustness with respect to mismatched signals and compare the WAS-ASB and the ASB;

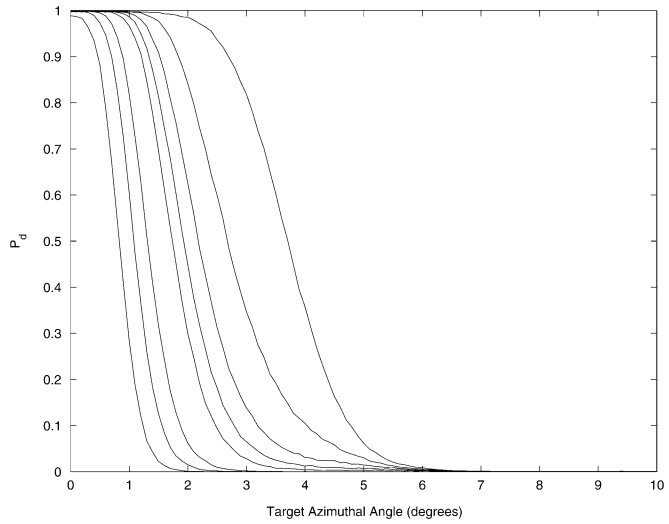

Fig. 6. P_d versus target azimuthal angle for the S-ASB with $N = 16$, $K = 32$, $r = 2$, and $\mathrm{SNR} = 19$ dB.

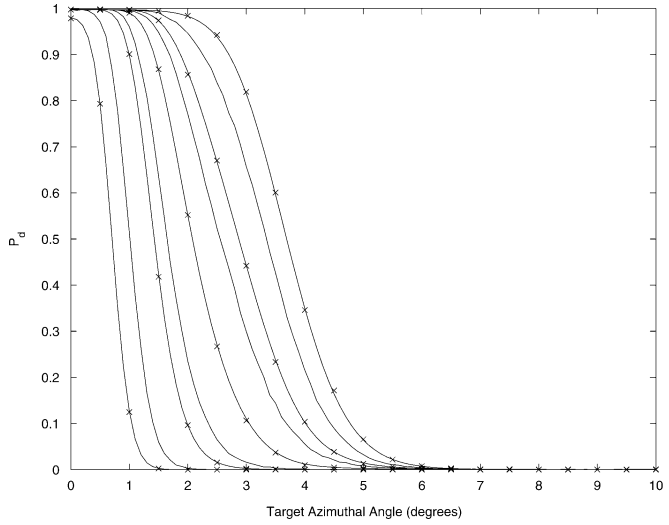

Fig. 7. P_d versus target azimuthal angle for the WAS-ASB with $N = 16$, $K = 32$, $r = 2$, and $\mathrm{SNR} = 19$ dB. Cross markers denote results obtained by Monte Carlo simulation.

again the plots show that the WAS-ASB can be made less sensitive to steering mismatches. In Fig. 10, we evaluate the capability to reject sidelobe targets and, to this end, we compare the WAS-ASB and the S-ASB (which differ in the second stage); as it can be seen, the WAS-ASB is generally superior to the S-ASB in rejecting mismatched signals.

In Figs. 11–13, we compare the WAS-ASB with the AMF-RAO for different values of N and K, and under the constraint that the loss with respect to Kelly's detector is less than (about) 1 dB for the perfectly matched case. Inspection of the figures highlights that the AMF-RAO is more sensitive than the WAS-ASB to the system parameters N and K. More precisely, the AMF-RAO becomes less selective as N and/or K increase and the WAS-ASB detector is slightly superior to the AMF-RAO in terms of selectivity for the system parameters considered in Figs. 12 and 13.

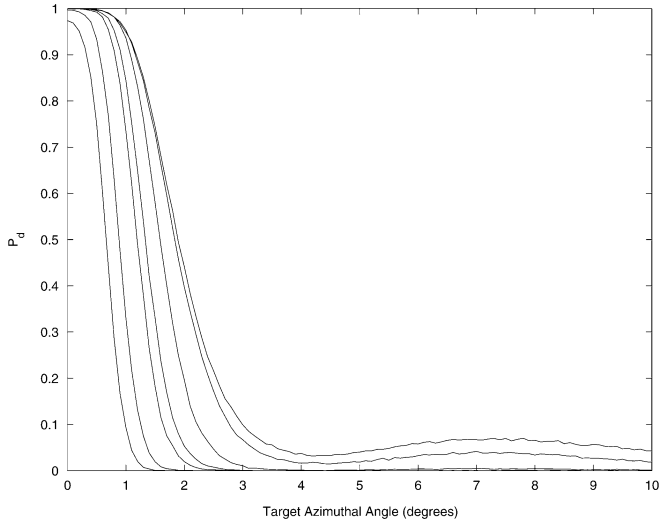

Fig. 8. P_d versus target azimuthal angle for the AMF-RAO with $N = 16$, $K = 32$, and $\mathrm{SNR} = 19$ dB.

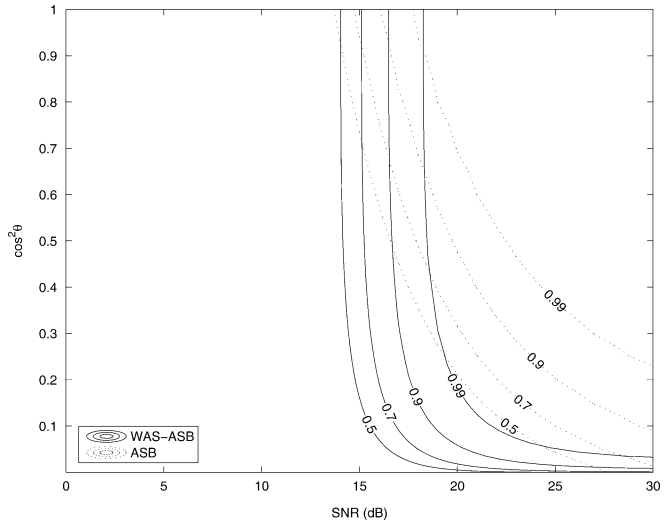

Fig. 9. Contours of constant P_d for the WAS-ASB and the ASB with $N = 16$, $K = 32$, $r = 2$, and threshold pairs corresponding to the most robust case.

As a final comment, observe that the WAS-ASB is more time consuming than the ASB and the AMF-RAO; note though that resorting to the usual Landau notation all of them are $O(KN^2)$, namely computation of their decision statistics requires a number of flops proportional to KN^2 (remember that $K \geq N$) which is in fact the number of flops required to evaluate $\boldsymbol{S}$.

V. Conclusion

We have proposed a two-stage detector consisting of a GLRT-based subspace detector followed by the W-ABORT. The performance analysis has been conducted analytically for both matched and mismatched signals. Although the proposed detector is not invariant to a meaningful group of transformations, it possesses the CFAR property with respect to the unknown covariance matrix of the noise and it can guarantee a wider range of directivity values with respect to its natural competitors. Thus, it appears as a viable means to trade detection performance of mainlobe targets for rejection capabilities

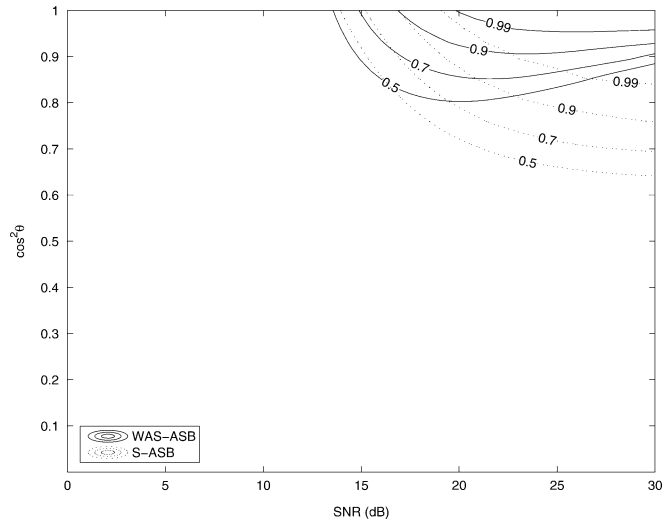

Fig. 10. Contours of constant P_d for the WAS-ASB and the S-ASB with $N = 16$, $K = 32$, $r = 2$, and threshold pairs corresponding to the most selective case.

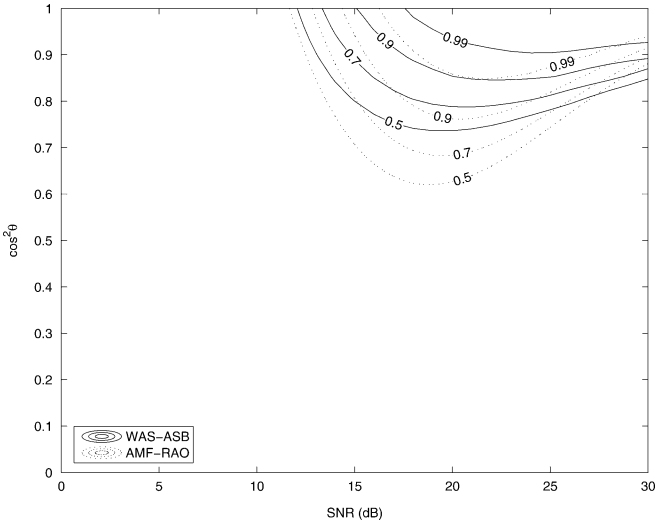

Fig. 12. Contours of constant P_d for the WAS-ASB and the AMF-RAO with $N = 16$, $K = 48$, $r = 2$, and threshold pairs corresponding to the most selective case.

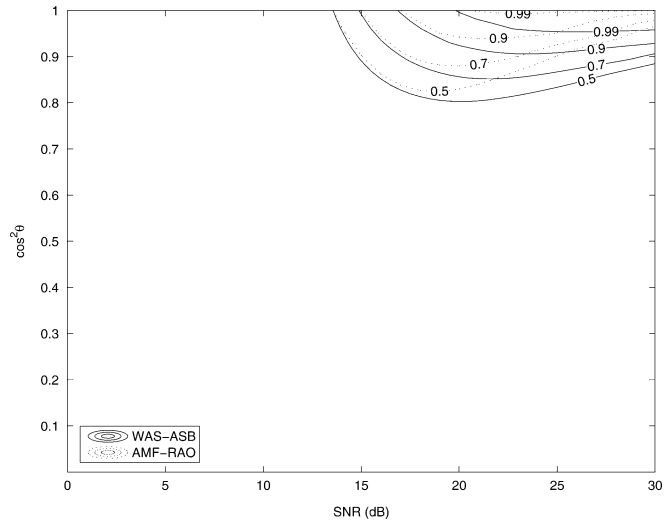

Fig. 11. Contours of constant P_d for the WAS-ASB and the AMF-RAO with $N = 16$, $K = 32$, $r = 2$, and threshold pairs corresponding to the most selective case.

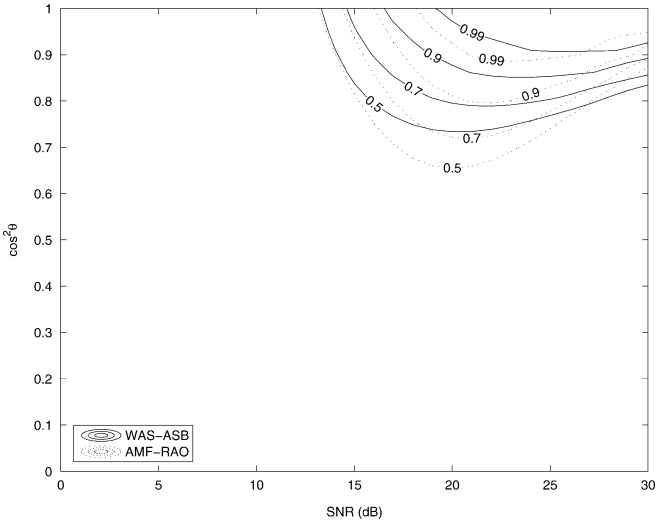

Fig. 13. Contours of constant P_d for the WAS-ASB and the AMF-RAO with $N = 30$, $K = 60$, $r = 2$, and threshold pairs corresponding to the most selective case.

of sidelobe ones. However, the design of flexible detection algorithms is still an open problem. Following the lead of [23], where the theory of convex optimization is used to provide flexibility for array beampattern synthesis, we are currently investigating the design of tunable receivers taking advantage of a stage aimed at adaptive weighting of the received signals.

Appendix A
Stochastic Representation of the SD and the W-Abort

In this section, we come up with suitable stochastic representations for $\tilde{t}_{\mathrm{SD}}$ and t_{WA}. As to the subspace detector, we refer to [22, App. A], where it is shown that

$$\tilde{t}_{\mathrm{SD}} = (\tilde{t}_{\mathrm{K}} + 1)(1 + c).$$

Now, let us concentrate on t_{WA} and note that

$$\begin{aligned} t_{\mathrm{WA}} &= \frac{1}{(t_{\mathrm{K}} - 1)^2(1 + \boldsymbol{z}^\dagger \boldsymbol{S}^{-1}\boldsymbol{z})} \\ &= \frac{|\boldsymbol{z}^\dagger \boldsymbol{S}^{-1}\boldsymbol{v}_0|^2}{(\boldsymbol{v}_0^\dagger \boldsymbol{S}^{-1}\boldsymbol{v}_0)(1 + \boldsymbol{z}^\dagger \boldsymbol{S}^{-1}\boldsymbol{z})} \frac{\boldsymbol{v}_0^\dagger \boldsymbol{S}^{-1}\boldsymbol{v}_0}{|\boldsymbol{z}^\dagger \boldsymbol{S}^{-1}\boldsymbol{v}_0|^2} \frac{1}{(t_{\mathrm{K}} - 1)^2} \\ &= \frac{t_{\mathrm{K}}}{t_{\mathrm{AMF}}(t_{\mathrm{K}} - 1)^2}, \end{aligned}$$

where

$$t_{\mathrm{AMF}} = \frac{|\boldsymbol{z}^\dagger \boldsymbol{S}^{-1}\boldsymbol{v}_0|^2}{\boldsymbol{v}_0^\dagger \boldsymbol{S}^{-1}\boldsymbol{v}_0}.$$

Now, let us define the following random variable

$$\beta = \frac{1}{1 + \boldsymbol{z}^\dagger \boldsymbol{S}^{-1}\boldsymbol{z} - t_{\mathrm{AMF}}}$$

and observe that

$$t_{\mathrm{AMF}} = \frac{\tilde{t}_{\mathrm{K}}}{\beta}.$$

It follows that t_{WA} can be recast as

$$t_{\mathrm{WA}} = (1 + \tilde{t}_{\mathrm{K}})\beta.$$

The above stochastic representation is useful to characterize the W-ABORT [24], but it has to be further modified in order to derive the statistical characterization of the overall two-stage detector. More precisely, we need to write the term β in a different form. To this end, applying the whitening transformation $\boldsymbol{R}^{-1/2}$ to the vectors $\boldsymbol{z}$ and $\boldsymbol{z}_k$, $k = 1, \ldots, K$, yields

$$\beta = \left(1 + \boldsymbol{z}_w^{\dagger}\boldsymbol{S}_w^{-1}\boldsymbol{z}_w - \frac{|\boldsymbol{z}_w^{\dagger}\boldsymbol{S}_w^{-1}\boldsymbol{v}_w|^2}{\boldsymbol{v}_w^{\dagger}\boldsymbol{S}_w^{-1}\boldsymbol{v}_w}\right)^{-1}$$

where $\boldsymbol{z}_w = \boldsymbol{R}^{-1/2}\boldsymbol{z}$, $\boldsymbol{v}_w = \boldsymbol{R}^{-1/2}\boldsymbol{v}_0$, and $\boldsymbol{S}_w = \boldsymbol{R}^{-1/2}\boldsymbol{S}\boldsymbol{R}^{-1/2}$; then, define a unitary matrix $\boldsymbol{U} \in \mathbb{C}^{N\times N}$ that rotates $\boldsymbol{H}_0$, which is a slice of unitary matrix obtained by means of QR factorization of the matrix $\boldsymbol{R}^{-1/2}\boldsymbol{H}$, into the first r elementary vectors, i.e.,

$$\boldsymbol{U}\boldsymbol{H}_0 = \begin{bmatrix} \boldsymbol{I}_r \\ \boldsymbol{0}_{(N-r)\times r} \end{bmatrix}$$

and, in particular,

$$\boldsymbol{U}\boldsymbol{R}^{-1/2}\boldsymbol{v}_0 = \sqrt{\boldsymbol{v}_0^{\dagger}\boldsymbol{R}^{-1}\boldsymbol{v}_0}\boldsymbol{e}_1.$$

It follows that β can be recast as

$$\beta = \left(1 + \boldsymbol{x}^{\dagger}\boldsymbol{S}_1^{-1}\boldsymbol{x} - \frac{|\boldsymbol{x}^{\dagger}\boldsymbol{S}_1^{-1}\boldsymbol{e}_1|^2}{\boldsymbol{e}_1^{\dagger}\boldsymbol{S}_1^{-1}\boldsymbol{e}_1}\right)^{-1} \tag{4}$$

where $\boldsymbol{x} = \boldsymbol{U}\boldsymbol{z}_w$ and $\boldsymbol{S}_1 = \boldsymbol{U}\boldsymbol{S}_w\boldsymbol{U}^{\dagger}$. Following the lead of [1] and [8], we decompose all vectors into two components: an A-component consisting of the first element only and a B-component consisting of the rest of the vector, namely as

$$\boldsymbol{x} = \begin{bmatrix} x_A \\ \boldsymbol{x}_B \end{bmatrix}, \boldsymbol{S}_1 = \begin{bmatrix} S_{1_{AA}} & \boldsymbol{S}_{1_{AB}} \\ \boldsymbol{S}_{1_{BA}} & \boldsymbol{S}_{1_{BB}} \end{bmatrix},$$

and

$$\boldsymbol{S}_1^{-1} = \begin{bmatrix} C_{AA} & \boldsymbol{C}_{AB} \\ \boldsymbol{C}_{BA} & \boldsymbol{C}_{BB} \end{bmatrix};$$

it follows that

$$\begin{aligned} \boldsymbol{x}^{\dagger}\boldsymbol{S}_1^{-1}\boldsymbol{x} &= (C_{AA}x_A + \boldsymbol{C}_{AB}\boldsymbol{x}_B)^{\dagger}C_{AA}^{-1} \\ &\quad \times (C_{AA}x_A + \boldsymbol{C}_{AB}\boldsymbol{x}_B) + \boldsymbol{x}_B^{\dagger}\boldsymbol{S}_{1_{BB}}^{-1}\boldsymbol{x}_B, \\ \boldsymbol{e}_1^{\dagger}\boldsymbol{S}_1^{-1}\boldsymbol{e}_1 &= C_{AA}, \\ \boldsymbol{x}^{\dagger}\boldsymbol{S}_1^{-1}\boldsymbol{e}_1 &= (C_{AA}x_A + \boldsymbol{C}_{AB}\boldsymbol{x}_B)^{\dagger}. \end{aligned}$$

Substituting the above equations into (4) yields

$$\beta = \frac{1}{1 + \boldsymbol{x}_B^{\dagger}\boldsymbol{S}_{1_{BB}}^{-1}\boldsymbol{x}_B}.$$

Again, let us partition the B-components into two subcomponents, a B_0-component containing the first $r-1$ elements and a B_1-component containing the rest of the B-vector

$$\boldsymbol{x}_B = \begin{bmatrix} \boldsymbol{x}_{B_0} \\ \boldsymbol{x}_{B_1} \end{bmatrix},$$

and

$$\boldsymbol{S}_{1_{BB}} = \begin{bmatrix} \boldsymbol{S}_{1_{B_0B_0}} & \boldsymbol{S}_{1_{B_0B_1}} \\ \boldsymbol{S}_{1_{B_1B_0}} & \boldsymbol{S}_{1_{B_1B_1}} \end{bmatrix}.$$

Now, by using equation A1-9 of [8], it is possible to show that $1 + \boldsymbol{x}_B^{\dagger}\boldsymbol{S}_{1_{BB}}^{-1}\boldsymbol{x}_B$ can be rewritten as

$$\begin{aligned} &\left(\boldsymbol{x}_{B_0} - \boldsymbol{S}_{1_{B_0B_1}}\boldsymbol{S}_{1_{B_1B_1}}^{-1}\boldsymbol{x}_{B_1}\right)^{\dagger} \\ &\quad \times \left(\boldsymbol{S}_{1_{B_0B_0}} - \boldsymbol{S}_{1_{B_0B_1}}\boldsymbol{S}_{1_{B_1B_1}}^{-1}\boldsymbol{S}_{1_{B_1B_0}}\right)^{-1} \\ &\quad \times \left(\boldsymbol{x}_{B_0} - \boldsymbol{S}_{1_{B_0B_1}}\boldsymbol{S}_{1_{B_1B_1}}^{-1}\boldsymbol{x}_{B_1}\right) \\ &\quad + 1 + \boldsymbol{x}_{B_1}^{\dagger}\boldsymbol{S}_{1_{B_1B_1}}^{-1}\boldsymbol{x}_{B_1} \\ &= (1+b)(1+c), \end{aligned}$$

where [see the equation shown at the bottom of the page]. Summarizing, we have found that t_{WA} can be written as

$$t_{\mathrm{WA}} = \frac{\tilde{t}_{\mathrm{K}} + 1}{(1+b)(1+c)}.$$

Appendix B
Statistical Characterization of b and c in Case of Mismatch

This section is devoted to the statistical characterization of the rv's b_θ and c_θ, i.e., the rv's b and c when the actual steering

$$c = \frac{\left(\boldsymbol{x}_{B_0} - \boldsymbol{S}_{1_{B_0B_1}}\boldsymbol{S}_{1_{B_1B_1}}^{-1}\boldsymbol{x}_{B_1}\right)^{\dagger}\left(\boldsymbol{S}_{1_{B_0B_0}} - \boldsymbol{S}_{1_{B_0B_1}}\boldsymbol{S}_{1_{B_1B_1}}^{-1}\boldsymbol{S}_{1_{B_1B_0}}\right)^{-1}\left(\boldsymbol{x}_{B_0} - \boldsymbol{S}_{1_{B_0B_1}}\boldsymbol{S}_{1_{B_1B_1}}^{-1}\boldsymbol{x}_{B_1}\right)}{1 + \boldsymbol{x}_{B_1}^{\dagger}\boldsymbol{S}_{1_{B_1B_1}}^{-1}\boldsymbol{x}_{B_1}}$$

and

$$b = \boldsymbol{x}_{B_1}^{\dagger}\boldsymbol{S}_{1_{B_1B_1}}^{-1}\boldsymbol{x}_{B_1}.$$

vector $\boldsymbol{p}$ and the nominal one $\boldsymbol{v}_0$ are not aligned. Under this hypothesis, the random vector $\boldsymbol{x}$ is distributed as [25]

$$\boldsymbol{x} \sim \mathcal{CN}_N \left(\alpha \sqrt{\boldsymbol{p}^\dagger \boldsymbol{R}^{-1} \boldsymbol{p}} \begin{bmatrix} e^{j\phi} \cos\theta \\ \boldsymbol{h}_{B_0} \sin\theta \\ \boldsymbol{h}_{B_1} \sin\theta \end{bmatrix}, \boldsymbol{I}_N \right)$$

where $\boldsymbol{h}_{B_0} \in \mathbb{C}^{(r-1)\times 1}$ and $\boldsymbol{h}_{B_1} \in \mathbb{C}^{(N-r)\times 1}$ are such that[2]

$$||\boldsymbol{h}_{B_0}||^2 + ||\boldsymbol{h}_{B_1}||^2 = 1$$

and

$$e^{j\phi} \cos\theta = \frac{\boldsymbol{v}_0^\dagger \boldsymbol{R}^{-1} \boldsymbol{p}}{\sqrt{\boldsymbol{p}^\dagger \boldsymbol{R}^{-1} \boldsymbol{p}} \sqrt{\boldsymbol{v}_0^\dagger \boldsymbol{R}^{-1} \boldsymbol{v}_0}}. \tag{5}$$

Now, recast c_θ as follows:

$$c_\theta = \boldsymbol{\nu}^\dagger \boldsymbol{G}^{-1} \boldsymbol{\nu}$$

where

$$\boldsymbol{\nu} = \frac{\boldsymbol{x}_{B_0} - \boldsymbol{S}_{1_{B_0 B_1}} \boldsymbol{S}_{1_{B_1 B_1}}^{-1} \boldsymbol{x}_{B_1}}{\sqrt{1 + b_\theta}}$$

and

$$\boldsymbol{G} = \boldsymbol{S}_{1_{B_0 B_0}} - \boldsymbol{S}_{1_{B_0 B_1}} \boldsymbol{S}_{1_{B_1 B_1}}^{-1} \boldsymbol{S}_{1_{B_1 B_0}};$$

following the rationale of the proof of Proposition 2 in [22], the following can be readily shown:

- $\boldsymbol{\nu}$ and $\boldsymbol{G}$ are each other independent;
- $\boldsymbol{G}$ is distributed according to the complex Wishart distribution with parameters $r-1$, $K-(N-1)+(r-1)$, and $\boldsymbol{I}_{r-1}$ (also conditionally on $\boldsymbol{S}_{1_{B_1 B_1}}$ and $\boldsymbol{x}_{B_1}$);
- given the B_1-components,

$$\boldsymbol{\nu} \sim \mathcal{CN}_{r-1} \left(\alpha \sqrt{\frac{\boldsymbol{p}^\dagger \boldsymbol{R}^{-1} \boldsymbol{p}}{1 + b_\theta}} \boldsymbol{h}_{B_0} \sin\theta, \boldsymbol{I}_{r-1} \right).$$

Therefore, by Theorem 1 in [22] we have that

$$c_\theta = \frac{\boldsymbol{\nu}^\dagger \boldsymbol{\nu}}{\boldsymbol{\nu}^\dagger \boldsymbol{\nu} / \boldsymbol{\nu}^\dagger \boldsymbol{G}^{-1} \boldsymbol{\nu}},$$

given b_θ, is ruled by the complex noncentral F-distribution with $r-1, K-N+2$ degrees of freedom and noncentrality parameter given by

$$\delta_{c_\theta}^2 = ||E[\boldsymbol{\nu}|b_\theta]||^2 = \frac{\mathrm{SNR}||\boldsymbol{h}_{B_0}||^2 \sin^2\theta}{1 + b_\theta}$$

where $E[\cdot]$ denotes statistical expectation. Theorem 1 in [22] comes in handy also to find the distribution of the rv b_θ; more precisely, note that, since $\boldsymbol{x}_{B_1} \sim \mathcal{CN}_{N-r}(\alpha \sqrt{\boldsymbol{p}^\dagger \boldsymbol{R}^{-1} \boldsymbol{p}} \quad \boldsymbol{h}_{B_1} \sin\theta, \boldsymbol{I}_{N-r})$ and $\boldsymbol{S}_{1_{B_1 B_1}} \sim \mathcal{CW}_{N-r}(K, \boldsymbol{I}_{N-r})$, random variable b_θ is ruled by the complex noncentral F-distribution with $N-r, K-N+r+1$ degrees of freedom and noncentrality parameter given by

$$\delta_{b_\theta}^2 = ||E[\boldsymbol{x}_{B_1}]||^2 = \mathrm{SNR}||\boldsymbol{h}_{B_1}||^2 \sin^2\theta.$$

[2] $||\cdot||$ denotes the Euclidean norm of a vector.

REFERENCES

[1] E. J. Kelly, "An adaptive detection algorithm," *IEEE Trans. Aerosp. Electron. Syst.*, vol. 22, no. 2, pp. 115–127, Mar. 1986.

[2] F. C. Robey, D. L. Fuhrman, E. J. Kelly, and R. Nitzberg, "A CFAR adaptive matched filter detector," *IEEE Trans. Aerosp. Electron. Syst.*, vol. 29, no. 1, pp. 208–216, Jan. 1992.

[3] S. Bose and A. O. Steinhardt, "A maximal invariant framework for adaptive detection with structured and unstructured covariance matrices," *IEEE Trans. Signal Process.*, vol. 43, no. 9, pp. 2164–2175, Sep. 1995.

[4] E. Conte, M. Lops, and G. Ricci, "Asymptotically optimum radar detection in compound Gaussian noise," *IEEE Trans. Aerosp. Electron. Syst.*, vol. 31, no. 2, pp. 617–625, Apr. 1995.

[5] L. L. Scharf and T. Mc Whorter, "Adaptive matched subspace detectors and adaptive coherence estimators," in *Proc. 30th Asilomar Conf. Signals Systems Computers*, Pacific Grove, CA, Nov. 3–6, 1996, pp. 1114–1117.

[6] S. Kraut, L. L. Scharf, and L. T. McWhorter, "Adaptive subspace detectors," *IEEE Trans. Signal Process.*, vol. 49, no. 1, pp. 1–16, Jan. 2001.

[7] S. Bose and A. O. Steinhardt, "Adaptive array detection of uncertain rank one waveforms," *IEEE Trans. Signal Process.*, vol. 44, no. 11, pp. 2801–2809, Nov. 1996.

[8] E. J. Kelly and K. Forsythe, "Adaptive detection and parameter estimation for multidimensional signal models," MIT, Lincoln Laboratory, Lexington, MA, Tech. Rep. No. 848, Apr. 19, 1989.

[9] N. B. Pulsone and C. M. Rader, "Adaptive beamformer orthogonal rejection test," *IEEE Trans. Signal Process.*, vol. 49, no. 3, pp. 521–529, Mar. 2001.

[10] G. A. Fabrizio, A. Farina, and M. D. Turley, "Spatial adaptive subspace detection in OTH radar," *IEEE Trans. Aerosp. Electron. Syst.*, vol. 39, no. 4, pp. 1407–1427, Oct. 2003.

[11] F. Bandiera, O. Besson, and G. Ricci, "An ABORT-like detector with improved mismatched signals rejection capabilities," *IEEE Trans. Signal Process.*, vol. 56, no. 1, pp. 14–25, Jan. 2008.

[12] A. De Maio, "Robust adaptive radar detection in the presence of steering vector mismatches," *IEEE Trans. Aerosp. Electron. Syst.*, vol. 41, no. 4, pp. 1322–1337, Oct. 2005.

[13] F. Bandiera, A. De Maio, and G. Ricci, "Adaptive CFAR radar detection with conic rejection," *IEEE Trans. Signal Process.*, vol. 55, no. 6, pp. 2533–2541, Jun. 2007.

[14] S. Z. Kalson, "An adaptive array detector with mismatched signal rejection," *IEEE Trans. Aerosp. Electron. Syst.*, vol. 28, no. 1, pp. 195–207, Jan. 1992.

[15] D. E. Kreithen and A. O. Steinhardt, "Target detection in post-stap undernulled clutter," presented at the 29th Annu. Asilomar Conf. Signals, Systems, Computers, Pacific Grove, CA, Nov. 1995.

[16] C. D. Richmond, "Statistical performance analysis of the adaptive sidelobe blanker detection algorithm," in *Proc. 31st Annu. Asilomar Conf. Signals, Systems, Computers*, Pacific Grove, CA, Nov. 1997.

[17] C. D. Richmond, "Performance of a class of adaptive detection algorithms in nonhomogeneous environments," *IEEE Trans. Signal Process.*, vol. 48, no. 5, pp. 1248–1262, May 2000.

[18] C. D. Richmond, "The theoretical performance of a class of space-time adaptive detection and training strategies for airborne radar," presented at the 32nd Annu. Asilomar Conf. Signals, Systems, Computers, Pacific Grove, CA, Nov. 1998.

[19] N. B. Pulsone and M. A. Zatman, "A computationally efficient two-step implementation of the GLRT," *IEEE Trans. Signal Process.*, vol. 48, no. 3, pp. 609–616, Mar. 2000.

[20] C. D. Richmond, "Performance of the adaptive sidelobe blanker detection algorithm in homogeneous environments," *IEEE Trans. Signal Process.*, vol. 48, no. 5, pp. 1235–1247, May 2000.

[21] A. De Maio, "Rao test for adaptive detection in Gaussian interference with unknown covariance matrix," *IEEE Trans. Signal Process.*, vol. 55, no. 7, pp. 3577–3584, Jul. 2007.

[22] F. Bandiera, D. Orlando, and G. Ricci, "A subspace-based adaptive sidelobe blanker," *IEEE Trans. Signal Process.*, vol. 56, no. 9, Sep. 2008.

[23] Y. Xie, J. Li, and J. Ward, "Adaptive weighting of signals via one matrix entity (AWESOME)," presented at the IEEE Radar Conf. 2007, Boston, MA, Apr. 17–20, 2007.
[24] F. Bandiera, O. Besson, D. Orlando, and G. Ricci, "Theoretical performance analysis of the W-ABORT detector," *IEEE Trans. Signal Process.*, vol. 56, no. 5, pp. 2117–2121, May 2008.
[25] E. J. Kelly, "Adaptive detection in non-stationary interference—Part III," MIT, Lincoln Laboratory, Lexington, MA, Tech. Rep. 761, Aug. 1987.

Francesco Bandiera (M'01) was born in Maglie, Lecce, Italy, on March 9, 1974. He received the Dr. Eng. Degree in computer engineering and the Ph.D. degree in information engineering from the University of Lecce (now University of Salento), Italy, in 2001 and 2005, respectively.

From July 2001 to February 2002, he has been with the University of Sannio, Benevento, Italy, engaged in a research project on mobile cellular telephony. Since December 2004, he has been an Assistant Professor with the Dipartimento di Ingegneria dell'Innovazione of the University of Salento, Lecce, Italy, where he is engaged in teaching and research. The main professional interests are in the field of statistical signal processing with more emphasis on radar signal processing, multiuser communications, and pollution detection on the sea surface based upon SAR imagery. He has held visiting positions with with the Electrical and Computer Engineering Department, University of Colorado at Boulder, CO (September 2003–March 2004), and with the Department of Avionics and Systems of ENSICA (now ISAE), Toulouse, France (October 2006).

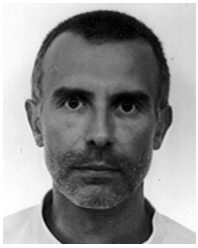

Olivier Besson (S'90–M'92–SM'04) received the Ph.D. degree in signal processing and the Habilitation à Diriger des Recherches degree, both from Institut National Polytechnique, Toulouse, France, in 1992 and 1998, resepectively.

He is currently a Professor with the Department of Electronics, Optronics and Signal of ISAE (Institut Supérieur de l'Aéronautique et de l'Espace), Toulouse, France. His research interests are in the general area of statistical signal and array processing, adaptive detection, space–time adaptive processing, and robust beamforming, mainly for radar applications.

Dr. Besson is a past member of the IEEE Sensor Array and Multichannel (SAM) Technical Committee and currently serves as an Associate Editor for the IEEE TRANSACTIONS ON SIGNAL PROCESSING.

Danilo Orlando was born in Gagliano del Capo, Italy, on August 9, 1978. He received the Dr. Eng. degree (with honors) in computer engineering and the Ph.D. degree in information engineering , both from the University of Salento, Italy, in 2004 and 2008, respectively.

Since July 2007, he collaborates with the University of Cassino, Italy, engaged in a research project on algorithms for track-before-detect of multiple targets in uncertain scenarios. He has held a visiting position with the Department of Avionics and Systems of ENSICA [now ISAE (Institut Supérieur de l'Aéronautique et de l'Espace)], Toulouse, France (February–March 2007). His main research interests are in the field of statistical signal processing with more emphasis on adaptive radar detection and tracking.

Giuseppe Ricci (M'01) was born in Naples, Italy, on February 15, 1964. He received the Dr. degree and the Ph.D. degree, both in electronic engineering, from the University of Naples Federico II, Italy, in 1990 and 1994, respectively.

Since 1995, he has been with the University of Lecce (now University of Salento), Italy, first as an Assistant Professor of Telecommunications and, since 2002, as a Professor. His research interests are in the field of statistical signal processing with emphasis on radar processing and CDMA systems. More precisely, he has focused on high-resolution radar clutter modeling, detection of radar signals in Gaussian and non-Gaussian disturbance, multiuser detection in overlay CDMA systems, and blind multiuser detection. He has held visiting positions at the University of Colorado at Boulder during 1997–1998 and in April–May 2001, where he has worked with Prof. M. K. Varanasi on blind multiuser detection, at the Colorado State University in July–September 2003 and March 2005, where he has worked with Prof. L. L. Scharf on radar detection of distributed targets, and at ENSICA [now ISAE (Institut Supérieur de l'Aéronautique et de l'Espace)], Toulouse, France, in March 2006, where he has worked with Prof. O. Besson on the derivation of adaptive direction detectors.